Biexciton emission and crystalline quality of ZnO nano-objects

2011 Nanotechnology 22 285710

(http://iopscience.iop.org/0957-4484/22/28/285710)

Nanotechnology **22** (2011) 285710 (7pp) doi:10.1088/0957-4484/22/28/285710

Biexciton emission and crystalline quality of ZnO nano-objects

Pierre Corfdir[1,4], Mohamed Abid[1,2], Anas Mouti[3], Pierre A Stadelmann[3], Elisa Papa[1], Jean-Philippe Ansermet[1], Jean-Daniel Ganière[1] and Benoît Deveaud-Plédran[1]

[1] Institute of Condensed Matter Physics, Ecole Polytechnique Fédérale de Lausanne (EPFL), 1015 Lausanne, Switzerland
[2] King Abdullah Institute of Nanotechnology, College of Science King Saud University, Riyadh 11451, Saudi Arabia
[3] Centre Interdisciplinaire de Microscopie Electronique, Ecole Polytechnique Fédérale de Lausanne (EPFL), 1015 Lausanne, Switzerland

E-mail: pierre.corfdir@epfl.ch

Received 22 March 2011, in final form 2 May 2011
Published 9 June 2011
Online at stacks.iop.org/Nano/22/285710

Abstract
The design of cost-effective standards for the quality of nano-objects is currently a key issue toward their massive use for optoelectronic applications. The observation by photoluminescence of narrow excitonic and biexcitonic emission lines in semiconductor nanowires is usually accepted as evidence for high structural quality. Here, we perform time-resolved cathodoluminescence experiments on isolated ZnO nanobelts grown by chemical vapor deposition. We observe narrow emission lines at low temperature, together with a clear biexciton line. Still, drastic alterations in both the CL intensity and lifetime are observed locally along the nano-object. We attribute these to non-radiative recombinations at edge dislocations, closing basal plane stacking faults, inhomogeneously distributed along the NB length. This leads us to the conclusion that the observation of narrow excitonic and biexcitonic emission lines is far from sufficient to grade the quality of a nano-object.

(Some figures in this article are in colour only in the electronic version)

1. Introduction

For the last ten years, chemically and physically synthesized nanostructures have attracted more and more attention from the scientific community as they represent archetypical building blocks for bottom-up nanotechnology [1]. The demonstration of nanowires' or nanobelts' (NBs) utilization in electronics [2], photonics [3] or biotechnology [4] has indeed opened a new avenue of research in the whole field of nanotechnology. Furthermore, compared to the traditional top-down approach that requires heavy lithography and deposition techniques, the bottom-up technology should be energy- and cost-effective. However, before mass production of such nanodevices, some standards are needed to grade the quality of the synthesized materials. Although x-ray diffraction and transmission electron microscopy (TEM) provide a very detailed insight into the material quality, as they can give access to the crystal structure and chemical composition, photoluminescence (PL) has the advantage to be a non-destructive method that requires no sample preparation. It is generally admitted that the quality of semiconductors is demonstrated when the PL spectrum is dominated by the near band-edge emission with excitonic transitions clearly resolved at cryogenic temperatures [5], the observation of biexcitonic emission being generally considered as one of the most conclusive criteria [6–8]. In the case of ZnO, the absence at 300 K of any emission band in the green spectral range is also admitted as an additional evidence of high material quality [9].

Here, we show that the usual PL experiments are not sufficient to ascertain the quality of nanostructures. We demonstrate that the information yielded by this technique might even be misleading, as it is averaged spatially over a few square microns. On the contrary, spatially resolved excitation techniques such as cathodoluminescence (CL) are ideal to

[4] Author to whom any correspondence should be addressed.

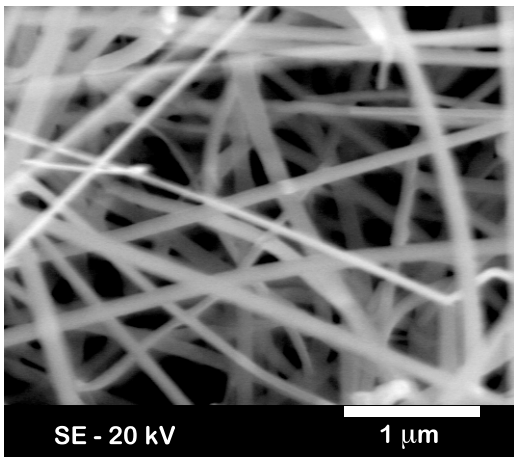

Figure 1. Secondary electron (SE) images on an ensemble of ZnO NBs grown by chemical vapor deposition. NBs are typically several micrometers or tens of micrometers long while their thickness is in the range 100–200 nm.

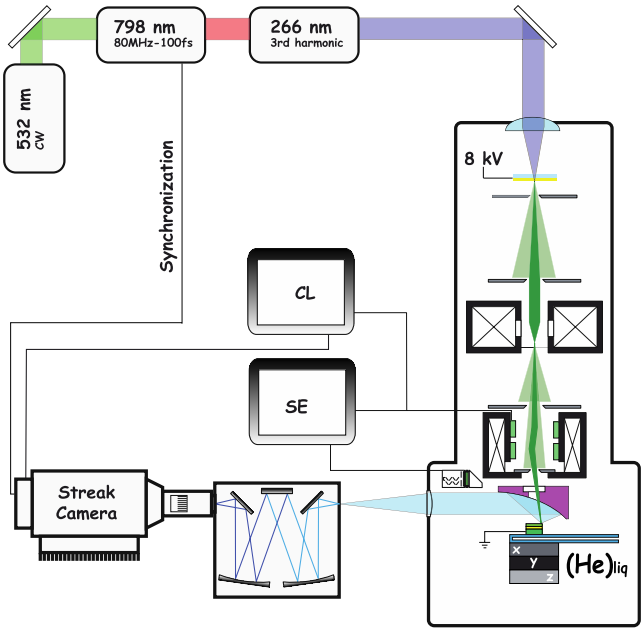

Figure 2. Time-resolved CL set-up. Electrons are extracted from a gold photocathode excited with the third harmonic of a pulsed Ti: Sapph. laser. The CL is collected with a parabolic mirror and sent to a monochromator and a streak camera for spectral and temporal analysis, respectively.

assess the local diffusion and recombination mechanisms of charge carriers in nano-objects. We concentrate here on the study by time-integrated (TI-) and time-resolved (TR-) CL of single ZnO nanobelts (NBs) elaborated by chemical vapor deposition. Although the overall high 'optical quality' of the sample is demonstrated by TR-CL through the observation of sharp excitonic and biexcitonic emission lines at 30 K together with the absence of any green emission band at room temperature, NBs present locally high basal stacking fault (BSF) densities. Through the measure of the local recombination lifetimes, we have access to the relative variation of internal quantum efficiency, along the length of the NB, and we show that the edge dislocations closing the BSFs open efficient non-radiative recombination paths for excitons.

2. Experimental details

The ZnO nanobelts (NBs) studied here have been grown by chemical vapor deposition (figure 1). A mixture of commercial ZnO and graphite powders (weight ratio 1:1) is grounded and loaded into a small alumina boat and then positioned at the center of the alumina tube. The latter is then evacuated to 2×10^{-2} Torr. The tube furnace is then heated to 1000 °C, and the pressure increased to 200 Torr with the Ar carrier gas flow rate set to 250 sccm (standard cubic centimeters per minute). The synthesis takes 30 min and the ZnO NBs form at temperatures typically comprised between 700 and 800 °C. The NBs are finally collected and dispersed on a n-doped silicon substrate to perform TR-CL on a single nano-object. Our TR-CL set-up consists of a scanning electron microscope (SEM) with an optically driven pulsed electron gun with 80.7 MHz repetition rate (figure 2) [10]. The pulses are accelerated along the column of the microscope and focused down to a 50 nm spot on the surface of the sample. In the present TI- and TR-CL experiments, the acceleration voltage and the probe current were set to 8 kV and 1 pA, respectively. Using the model of Bonard *et al* [11], we estimate to 150 nm the maximum lateral extension of the generation volume in the NB[5]. The CL is then collected by a parabolic mirror and sent to a monochromator and a streak camera for spectral and temporal analyses. Measurements can be carried out between 30 and 300 K and the overall time resolution of the set-up is 10 ps. The micrograph of the ensemble of ZnO NBs shown in figure 1 has been taken with a JEOL 7001 F field effect gun SEM working at 20 kV. Finally, high-resolution TEM has been performed with a JEOL 2200 FS with the acceleration voltage set to 200 kV.

3. Results and discussion

Figure 3(a) shows CL spectra of a single ZnO NB for temperatures comprised between 30 and 120 K, when excitation is delivered at the extremity of the NB (hereafter called Region (1), see figure 4(a)). The emission at 30 K is dominated by two transitions at 3.362 and 3.371 eV. We observe at 3.381 eV a shoulder on the high-energy side of the 3.371 eV line. The quenching of the emission at 3.371 eV to the benefit of that at 3.381 eV allows us to attribute them to the recombination of donor bound excitons A ($D^{\circ}X_A$) and free excitons A (X_A), respectively. The 10 meV energy separation between $D^{\circ}X_A$ and X_A agrees with the experimental values of $D^{\circ}X_A$ binding energy reported by other groups [13]. Assuming that the electron and hole effective mass are $m_e = 0.24m_0$ and $m_h = 0.78\ m_0$ [14], and that the background dielectric constant is $\varepsilon_b = 6.2$ [15], we obtain a $D^{\circ}X_A$ binding energy of 9.4 meV [16], which is also in good agreement with our results.

[5] We used the set of parameters proposed for GaN by [12].

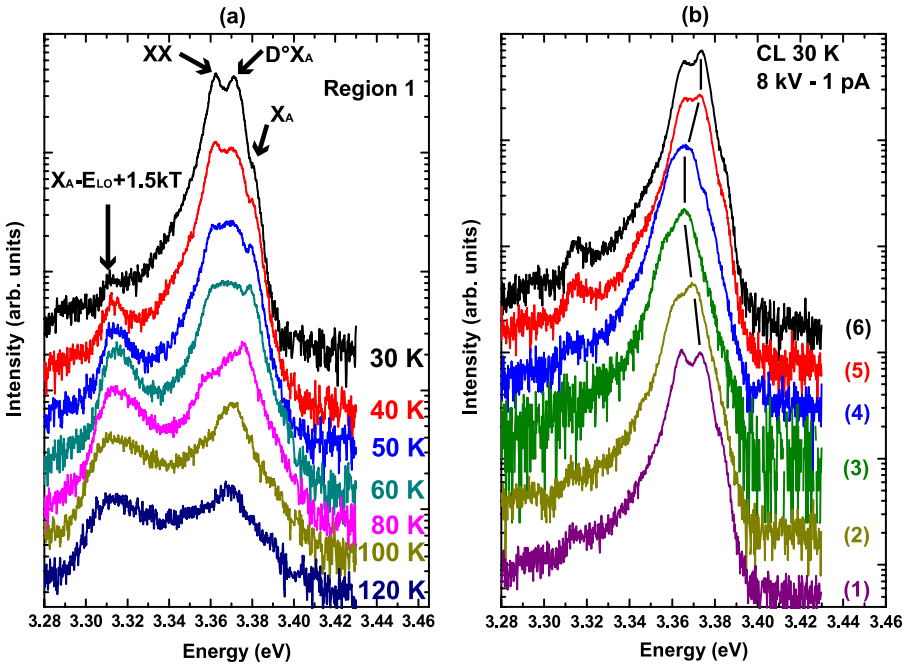

Figure 3. (a) Time-integrated CL spectra with respect to temperature when excitation is delivered at one extremity of the NB (Region (1)). The spectra have been shifted vertically for clarity. (b) Evolution of time-integrated CL spectra of the ZnO NB at 30 K along the NB axis. The spectra have been shifted vertically. Together with the redshift of the emission in the vicinity of Regions (3), (4), the emission lines get broadened.

Above 100 K, we also observe a kink in the high-energy side of the X_A emission, which we attribute to the thermal activation of exciton B luminescence (X_B). Note that even at 300 K, the near band-edge emission dominates the emission spectrum and we hardly record any signal from the green band centered at 2.3 eV (figure 5). This emission band, observed in bulk as well as in ZnO nano-objects, is commonly attributed to the recombination of donor–acceptor pairs constituted by a deep acceptor and a shallow donor [17]. However, to our knowledge, the origin of the deep acceptor has not been ascertained yet and could depend on the growth conditions [18]. A weaker emission band centered at 3.313 eV at 30 K is also observed and we attribute it to the first LO phonon replica of exciton A. When T is increased, the peak emission energy of this band indeed follows $E_{XA} - E_{LO} + 1.5kT$, where E_{XA} is the exciton A energy and $E_{LO} = 72$ meV is the LO phonon energy [19]. Compared to bulk ZnO layers, we note that the X_A-LO emission intensity at 120 K with respect to the zero-phonon line is rather strong (figure 3(a)). We attribute such a feature to the alteration by the nanobelt geometry of both electron and hole coupling strengths with the phonon, as recently proposed in [20].

Concerning the 3.362 eV line, its emission intensity quenches faster with temperature than the emission from $D^\circ X_A$, indicating that this line does not arise from excitons bound to deeper impurities. Such a deeper bound exciton would have indeed exhibited a less efficient thermal detrapping than $D^\circ X_A$ [21]. The time dependences at 30 K of the CL at 3.313, 3.362, 3.371 and 3.381 eV are plotted in figure 6(a). $D^\circ X_A$, X_A and X_A-LO intensities all decay exponentially with the characteristic time $\tau_{eff,X} = 255$ ps, attesting of efficient thermalization between these free and donor bound exciton distributions. The CL at 3.362 eV decays with an effective decay time $\tau_{eff,XX} = 120$ ps, i.e. approximately two times faster than $D^\circ X_A$ and X_A PL. As the deeper the localization, the longer the radiative lifetime [22], we definitely exclude that the 3.362 eV line could arise from any localized exciton state. On the contrary, such a fast decay is typical of biexciton recombination. Within the excitonic molecule model, a biexciton can be seen as two Wannier excitons that execute a correlated motion [23]. The transition dipole involved in the recombination of a biexciton involves only one of the excitons constituting the exciton molecule [24]. The biexciton recombination energy E_{XX} is thus given by $E_{XA} - E_{B,XX}$, where $E_{B,XX}$ is the biexciton binding energy and where we have neglected biexciton kinetic energy. At thermodynamic equilibrium, exciton and biexciton densities N_X and N_{XX} follow the mass action law:

$$\frac{N_X^2}{N_{XX}} \propto kT \,\mathrm{Exp}\left[-\frac{E_{B,XX}}{kT}\right]. \qquad (1)$$

This mass action law between excitons and biexcitons has been derived from that describing the equilibrium between excitons and free electron hole pairs, as described in [25, 26]. Consequently, in a time-resolved experiment, once excitons and biexcitons are thermalized, the evolution with time of their respective emission intensities I_X and I_{XX} obey $I_X^2(t) \propto I_{XX}(t)$ [27]. The time decay curves of the 3.362 eV CL and of the exciton CL squared are plotted in figure 6(b) and clearly attest to the presence of biexcitons in our nano-object. We deduce $E_{B,XX} = 19$ meV, which is in good agreement with previous reports made on bulk [28] and nanocolumnar

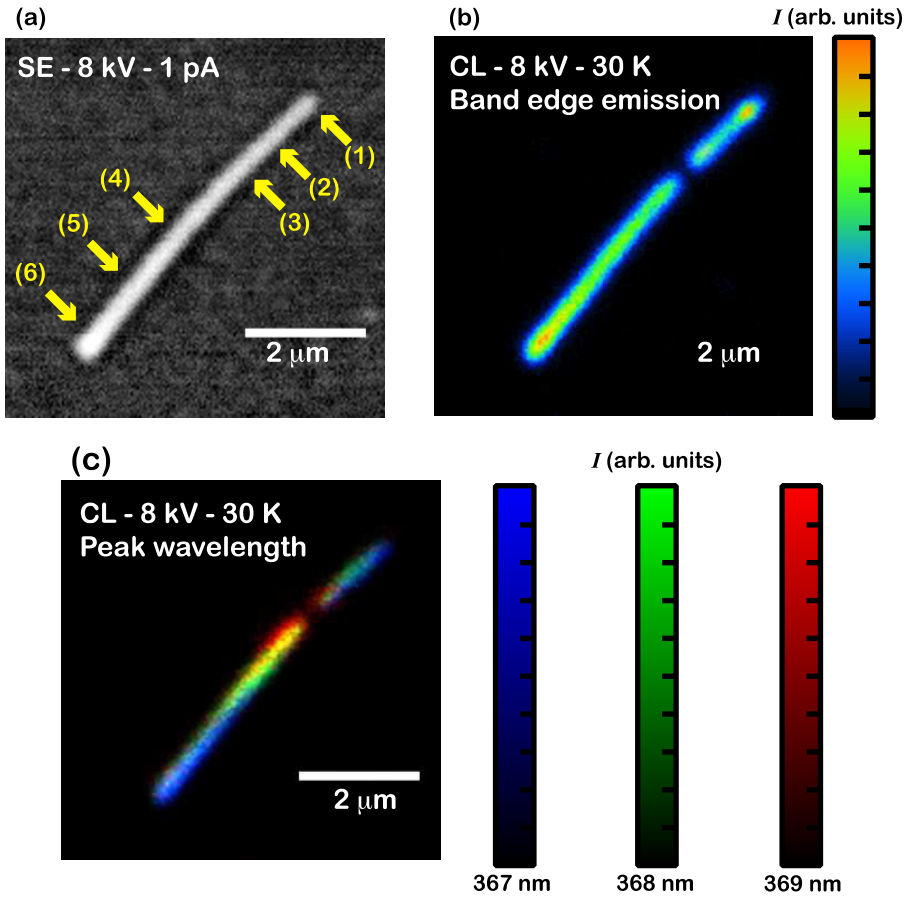

Figure 4. (a) Secondary electron (SE) image of the investigated NB taken with our homemade pulsed electron gun. Yellow arrows show the regions of the sample where time-resolved and time-integrated experiments were performed. The NB is slightly bent between Regions (3) and (4). (b) Time-integrated CL mapping of the NB at 30 K. The signal has been spectrally integrated between 3.34 and 3.40 eV. A drastic drop in CL intensity is observed in Region (3). (c) Local peak CL wavelength at 30 K. Compared to Regions (1) and (6), the NB emission is red-shifted when excitation is delivered in the vicinity of Region (3).

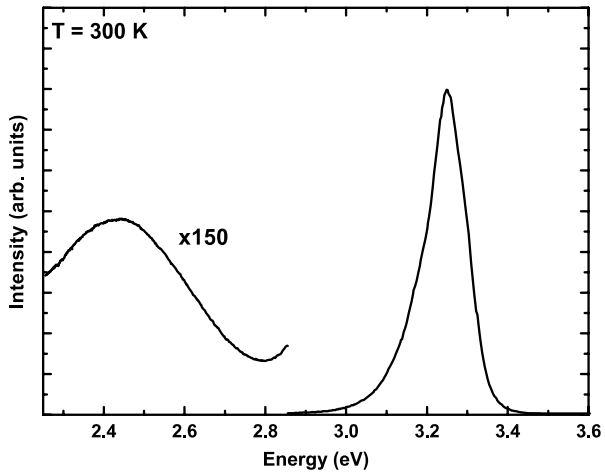

Figure 5. Continuous-wave cathodoluminescence spectrum of the investigated NB at 300 K when excitation is delivered in Region (1). The near band-edge emission still dominates the CL spectrum at room temperature.

ZnO [6–8]. As pointed out by Yamamoto *et al* [28], we note however that the experimental value of $E_{B,XX}$ is quite large compared to the one predicted by the variational method [29].

So far, we have observed that, at low-temperatures, the ZnO NB mainly exhibits intense and narrow emissions from donor bound and free excitons, and we have also attested the observation of biexcitons (regions (1), (2), (5) and (6) in figure 4(a)). Still, as shown in figures 4(b) and (c), the NB emission intensity and peak emission energy are not constant along its axis. Compared to the $D^{\circ}X_A$ emission energy in Region (1), we observe a 10 meV redshift of the NB peak emission energy in Region (3). Interestingly, such a huge redshift is observed where the NB is slightly bent, indicating some variation in strain state in that region [30]. In parallel, the emission linewidth in Region (3) is increased, and one cannot separate the X_A and $D^{\circ}X_A$ emissions anymore. More importantly, the effective CL decay time is reduced in Region (3) compared to what is observed in Regions (1) and (6) (figure 7), while the CL intensity at zero delay is almost position independent. As the time evolution of the exciton emission intensity is given by

$$I_{CL}(t) \propto \frac{1}{\tau_r} \mathrm{Exp}\left[-t \Big/ \left(\frac{1}{\tau_r} + \frac{1}{\tau_{nr}}\right)^{-1}\right], \qquad (2)$$

with τ_r and τ_{nr} radiative and non-radiative lifetimes, respectively, we conclude that charge carriers suffer from

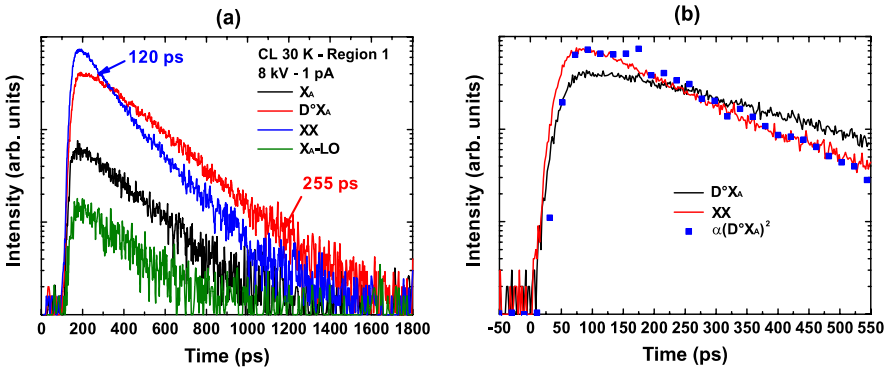

Figure 6. (a) Free exciton X_A, donor bound exciton $D^\circ X_A$, biexciton XX and free exciton first LO phonon replica X_A–LO CL decays (black, red, blue and green curves, resp.) taken at 30 K with excitation delivered in Region (1). X_A, $D^\circ X_A$ and X_A-LO exhibit the same decay, attesting to efficient thermalization mechanisms. (b) The 3.362 eV CL transient quadratically follows that of X_A and $D^\circ X_A$, evidencing its biexcitonic origin.

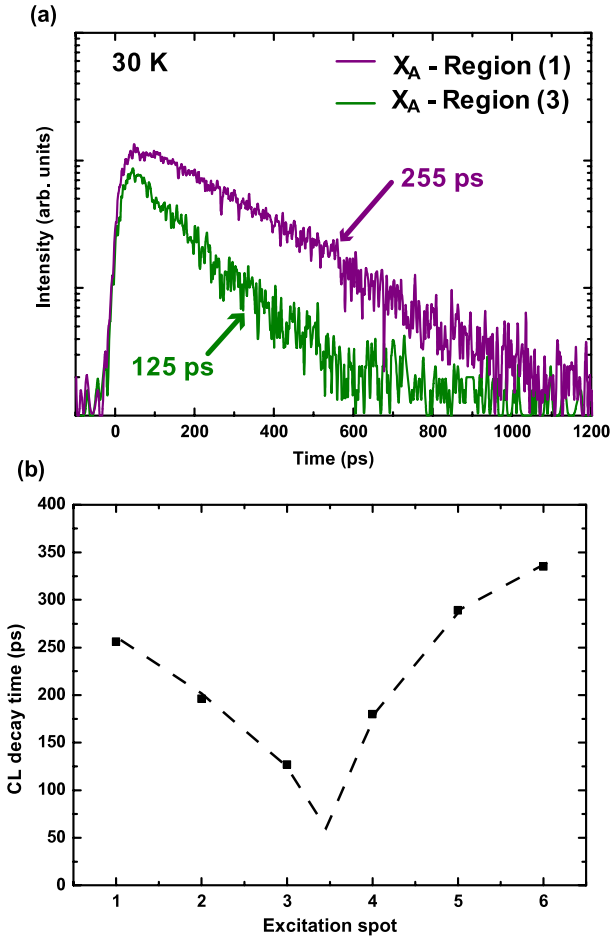

Figure 7. (a) Free exciton CL transients taken at 30 K when excitation is delivered on Regions (1) and (3) (magenta and green curves, resp.). (b) Effective X_A CL decay time along the NB length (squares). Dashed lines are guides to the eye. In the vicinity of Region (3), X_A CL decays faster. Combined with the constancy of the initial CL intensity wherever the excitation is delivered, such an observation evidences efficient non-radiative recombinations in Region (3) of the NB.

efficient non-radiative recombinations in Region (3). It is worth underlining that the most intense contribution to the luminescence of the sample comes from the regions where the emission lines are narrow (figures 3(b) and 4(b)). As a consequence, a PL spectrum obtained on such a NB would have been dominated by the emission from both ends of the NB. The observation of narrow excitonic emission at low temperature and *a fortiori* the recombination of biexcitons would have then led to the conclusion that the structure is of high quality and that the growth method used here is appropriate for technological application, which is totally incorrect regarding the experimental results displayed in figures 3(b), 4 and 7.

While the TR-CL measurements presented above allowed a conclusion on the non-radiative character of the recombination centers in Regions (3) and (4), we performed TEM on a similar NB to assess their structural origin. As shown in figure 8, we observe basal plane stacking faults (BSFs) perpendicular to the NB length (*c*-axis) and closed by edge dislocations. In ZnO, BSFs are radiative and give rise at low temperatures to an emission band centered at 3.31 eV [31] and can be modeled as three monolayers thick type-II QWs of cubic-like ZnO embedded in the hexagonal matrix [32]. Although BSFs are closed either by partial dislocations or prismatic stacking faults that both act as non-radiative recombination centers [33, 34], intra-BSF localization mechanisms [35] combined with the fact that in bulk material BSFs can extend over several microns, usually allow for the observation of intense emission from BSFs. On the contrary, the typical extension of BSFs in our NBs is a few tens of nm (figure 8), which is much shorter than the exciton diffusion length in ZnO [36]. Thus, in NBs, BSFs-excitons can be trapped efficiently by the non-radiative defects closing the BSFs, before they recombine radiatively. For this reason, we do not detect any CL whose time and temperature dependences could be characteristic of BSF-related emission (figure 3). From the considerations above, we propose that the non-radiative recombination centers detected in the vicinity of Region (3) could arise from high local density in BSFs. Moreover, we note that the excitonic bandgap in Regions (1) and (6) is blueshifted compared to that of unstrained ZnO [37]. The presence of bundles of BSFs is therefore consistent with the strain relaxation observed when scanning the NB CL from Regions (1) or (6) to Region (3) (figure 3(b)).

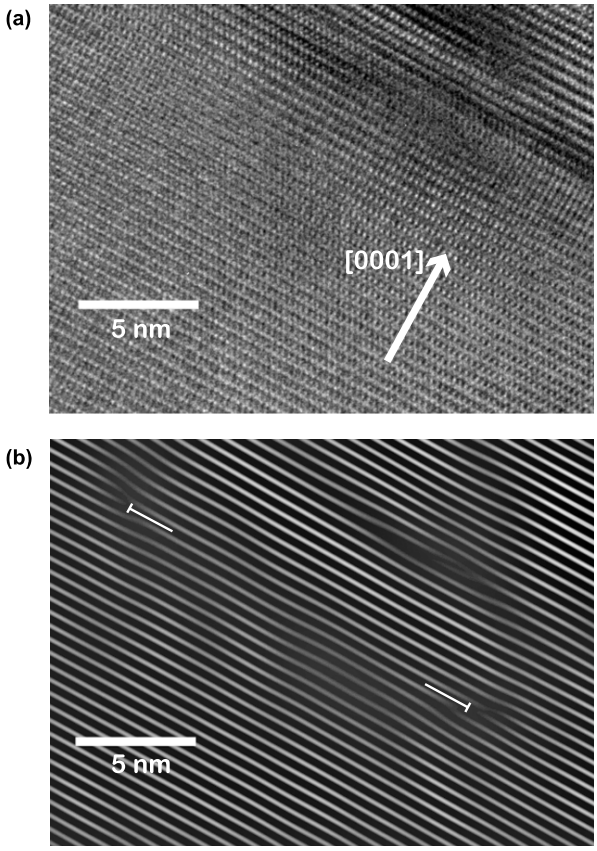

Figure 8. (a) High-resolution TEM image along the $[2\bar{1}\bar{1}0]$ direction taken on a ZnO NB. (b) Result of Fourier filtering of (a) using the (0002) reflection to evidence the presence of dislocations. A basal plane stacking fault is enclosed by two edge dislocations.

4. Conclusions

In conclusion, our experiments demonstrate the inefficiency of usual PL techniques to probe the dynamics of charge carriers in ZnO and more generally in semiconductor nanostructures. We emphasize that the observation of narrow excitonic and biexcitonic lines are not satisfactory to assess the quality of a nano-object, when devoted for optoelectronics applications. On the contrary, CL techniques seem more satisfactory as their localized excitation enables the characterization of recombination mechanisms at the nanometer-scale. We believe it is mandatory to couple a TR-CL set-up, which provides a direct mapping of the internal quantum efficiency, with a CL set-up coupled with a scanning TEM, allowing correlation of the optical properties of a nanostructure with the structural ones [38]. More generally, this work is part of the current research on the peculiar emission properties of semiconductor nanostructures compared to thick layers. While it has been recently shown that the low-temperature emission from ensemble of strain- and defect-free semiconductor nanowires of a diameter typically below 50 nm was intrinsically broad due to surface effects [21, 39], the present work demonstrates that it is not possible to extend to nanostructures the commonly accepted optical signatures of high quality used for bulk material. We thus strongly recommend not using general terms such as 'optical quality', when grading nanostructures dedicated for optoelectronics.

Acknowledgments

We thank the *Attolight* Company for the constant improvement of the TR-CL set-up, R Rochat, N Leiser, Y Trolliet and D Trolliet for technical assistance. We also acknowledge financial support from the Swiss National Science Foundation Project No. 119840 and from the Swiss NCCR Quantum Photonics.

References

[1] Lieber C M and Wang Z L 2007 *MRS Bull.* **32** 99–108
[2] Huang Y, Duan X, Cui Y, Lauhon L J, Kim K H and Lieber C M 2001 *Science* **294** 1313–7
[3] Huang M H, Mao S, Feick H, Yan H, Wu Y, Kind H, Weber E, Russo R and Yong P 2001 *Science* **292** 1897–9
[4] Cui Y, Wei Q, Park H and Lieber C M 2001 *Science* **293** 1289–92
[5] Park W I, Kim D H, Jung S W and Yi G C 2002 *Appl. Phys. Lett.* **80** 4232–4
[6] Zhang B P, Binh N T, Segawa Y, Wakatsuki K and Usami N 2003 *Appl. Phys. Lett.* **83** 1635–7
[7] Zhang B P, Binh N T, Segawa Y, Kawashiba Y and Haga K 2004 *Appl. Phys. Lett.* **84** 586–8
[8] Kim S W, Fujita S and Fujita S 2005 *Appl. Phys. Lett.* **86** 153119
[9] Park W I, Yi G C, Kim M Y and Pennycook S J 2002 *Adv. Mater.* **14** 1841–3
[10] Merano M *et al* 2005 *Nature* **438** 479–82
[11] Bonard J M and Ganière J D 1996 *J. Appl. Phys.* **79** 6987–94
[12] Parish C M and Russell P E 2006 *Appl. Phys. Lett.* **89** 192108
[13] Park W I, Sun Y H, Jung S W and Yi G C 2003 *Appl. Phys. Lett.* **82** 964–6
[14] Coli G and Bajaj K K 2001 *Appl. Phys. Lett.* **78** 2861–3
[15] Lagois J 1981 *Phys. Rev.* B **23** 5511–20
[16] Suffczynski M and Wolniewicz L 1989 *Phys. Rev.* B **40** 6250–7
[17] Reynolds D C, Look D C and Jogai B 2001 *J. Appl. Phys.* **89** 6189–91
[18] Heo Y W, Norton D P and Pearton S J 2005 *J. Appl. Phys.* **98** 073502
[19] Wang L and Giles N C 2003 *J. Appl. Phys.* **94** 973–8
[20] Feldtmann T, Kira M and Koch S W 2010 *J. Lumin.* **130** 107–13
[21] Corfdir P, Lefebvre P, Ristić J, Valvin P, Calleja E, Ganière J D and Deveaud-Plédran B 2009 *J. Appl. Phys.* **105** 013113
[22] Rashba E I and Gurgenishvili G E 1962 *Fiz. Tverd. Tela (Leningrad)* **4** 759–60
Rashba E I and Gurgenishvili G E 1962 *Sov. Phys.—Solid State* **4** 759–60 (Engl. Transl.)
[23] Citrin D S 1994 *Phys. Rev.* B **50** 17655–8
[24] Hanamura E 1975 *J. Phys. Soc. Japan* **39** 1516–24
[25] Chemla D S 1983 *Helv. Phys. Acta* **56** 607–37
[26] Colocci M, Gurioli M and Vinattieri A 1990 *J. Appl. Phys.* **68** 2809–12
[27] Kim J C, Wake D R and Wolfe J P 1994 *Phys. Rev.* B **50** 15099–107
[28] Yamamoto A, Miyajima K, Goto T, Ko H J and Yao T 2001 *J. Appl. Phys.* **90** 4973–6

[29] Usukara J, Suzuki Y and Varga K 1999 *Phys. Rev.* B **59** 5652–61
[30] Han X B *et al* 2009 *Adv. Mater.* **21** 4937–41
[31] Schirra M, Schneider R, Reiser A, Prinz G M, Feneberg M, Biskupek J, Kaiser U, Krill C E, Thonke K and Sauer R 2008 *Phys. Rev.* B **77** 125215
[32] Yan Y, Dalpian G M, Al-Jassim M M and Wei S H 2004 *Phys. Rev.* B **70** 193206
[33] Wu Z H, Fischer A M, Ponce F A, Bastek B, Christen J, Wernicke T, Weyers M and Kneissl M 2008 *Appl. Phys. Lett.* **92** 171904
[34] Corfdir P, Lefebvre P, Levrat J, Dussaigne A, Ganière J D, Martin D, Ristić J, Zhu T, Grandjean N and Deveaud-Plédran B 2009 *J. Appl. Phys.* **105** 043102
[35] Corfdir P, Lefebvre P, Ristić J, Ganière J D and Deveaud-Plédran B 2009 *Phys. Rev.* B **80** 153309
[36] Yoo J, Yi G C and Dang L S 2008 *Small* **4** 467–70
[37] Gil B 2001 *Phys. Rev.* B **64** R201310
[38] Lim S K, Brewster M, Qian F, Li Y, Lieber C M and Gradecak S 2009 *Nano Lett.* **9** 3940–4
[39] Brandt O, Pfüller C, Chèze C, Geelhaar L and Riechert H 2010 *Phys. Rev.* B **81** 045302